Numerical Heat Transfer, Part B, 51: 391–409, 2007

ISSN: 1040-7790 print/1521-0626 online
DOI: 10.1080/10407790600964583

Taylor & Francis
Taylor & Francis Group

SECOND-ORDER RADIATIVE TRANSFER EQUATION AND ITS PROPERTIES OF NUMERICAL SOLUTION USING THE FINITE-ELEMENT METHOD

J. M. Zhao and L. H. Liu
School of Energy Science and Engineering, Harbin Institute of Technology, People's Republic of China

The original radiative transfer equation is a first-order integrodifferential equation, which can be taken as a convection-dominated equation. The presence of the convection term may cause nonphysical oscillation of solutions. This type of instability can occur in many numerical methods, including the finite-difference method and the finite-element method, if no special stability treatment is used. To overcome this problem, a second-order radiative transfer equation is derived, which is a diffusion-type equation similar to the heat conduction equation for an anisotropic medium. The consistency of the second-order radiative transfer equation with the original radiative transfer equation is demonstrated. The perturbation characteristics of error are analyzed and compared for both the first- and second-order equations. Good numerical properties are found for the second-order radiative transfer equation. To show the properties of the numerical solution, the standard Galerkin finite-element method is employed to solve the second-order radiative transfer equation. Four test problems are taken as examples to check the numerical properties of the second-order radiative transfer equation. The results show that the standard Galerkin finite-element solution of the second-order radiative transfer equation is numerically stable, efficient, and accurate.

INTRODUCTION

Numerical solution of the radiative transfer in an absorbing, emitting, and scattering medium requires considerable effort for most practical systems composed of semitransparent media. Recently, many numerical methods have been developed to solve the problems of radiative heat transfer in semitransparent media. The solution methods may mainly be classified into two classes: (1) the methods based on ray tracing, such as the zonal method [1] and the Monte Carlo method [2, 3]; and (2) the methods based on the discretization of a standard form or variation of the radiative transfer equation (RTE), such as the discrete-ordinates method (DOM) [3–15], the finite-volume method (FVM) [16–23], and the finite-element method (FEM) [24–29]. The ray-tracing-based methods do not rely explicitly on the RTE. The simulation processes of these methods are numerical stable and have clear

Received 15 June 2006; accepted 27 July 2006.
The support of this work by the National Nature Science Foundation of China (50425619, 50336010) is gratefully acknowledged.
Address correspondence to L. H. Liu, School of Energy Science and Engineering, Harbin Institute of Technology, 92 West Dazhi Street, Harbin 150001, People's Republic of China. E-mail: lhliu@hit.edu.cn

NOMENCLATURE

A_{out}	error amplifying factor of outflow boundary condition
$A_{S,1\text{st}}$	error amplifying factor of radiative source term based on the original RTE
$A_{S,2\text{nd}}$	error amplifying factor of radiative source term based on the SORTE
E^{int}	integral averaged relative error
$E^{\text{int}}_{\text{out}}$	integral averaged relative error caused by the perturbation at outflow boundary condition
$E^{\text{int}}_{S,1\text{st}}$	integral averaged relative error caused by the perturbation of radiative source term based on the original RTE
$E^{\text{int}}_{S,2\text{nd}}$	integral averaged relative error caused by the perturbation of radiative source term based on the SORTE
$E^{\text{int}}_{S,1\text{st}}$	integral averaged relative error caused by the perturbation of radiative source term based on the original RTE
$E^{\text{rel}}_{\text{in}}$	relative perturbation error function of inflow boundary condition
$\mathbf{H}$	matrix defined in Eq. (47)
I	radiative intensity, $\text{W/m}^2\,\text{sr}$
$\mathbf{I}$	vector of radiative intensity
$\mathbf{K}$	stiff matrix defined in Eq. (46)
L	length of the ray trajectories considered, side length of rectangular enclosure
M	number of discrete ordinate direction
$\mathbf{n}$	inward normal vector
N_{sol}	total number of solution nodes
q	radiative heat flux, W/m^2
$\mathbf{r}$	spatial coordinates vector
s	ray trajectory coordinate
S	source function defined in Eq. (5)
T	temperature, K
u	arbitrary function in a function space
V	computational domain
w	weight of discrete ordinate direction
x, y, z	Cartesian coordinates
β	extinction coefficient $(= \kappa_a + \kappa_s)$, m^{-1}
Γ	boundary
Γ_D	inflow boundary, Dirichlet boundary
Γ_N	outflow boundary, Neumann boundary
ε	perturbation error
ε_w	wall emissivity
κ_a	absorption coefficient, m^{-1}
κ_s	scattering coefficient, m^{-1}
μ, ξ, η	Cartesian components of Ω
σ	Stefan-Boltzmann constant, $\text{W/m}^2\,\text{K}^4$
τ	optical coordinate
τ_L	optical thickness $(= \beta L)$
τ_x, τ_y, τ_z	optical coordinates $(\tau_x = \beta x, \tau_y = \beta y, \tau_z = \beta z)$
$\bar{\tau}$	normalized optical coordinate defined in Eq. (15)
ϕ	shape function
Φ	scattering phase function
ω	scattering albedo
Ω, Ω'	vector of radiation direction
Ω	solid angle

Subscripts

b	black body
g	medium
i, j	spatial node index
w	value at wall
0	inflow

Superscripts

m, m'	the mth discrete ordinate direction

physical meaning. However, they are often too time-consuming even for relatively simple problems, thus the second class of methods has received considerable attention for its advantages, such as being easy and flexible to deal with the multidimensional problems of radiative heat transfer.

In the second class of methods, traditional methods such as the DOM, FVM, and FEM are often based on the original RTE, which is a first-order integrodifferential equation and can be taken as a convection-dominated equation. The presence of a convection term may cause nonphysical oscillation of solutions. This type of instability can occur in many numerical methods, including the finite-difference method and the finite-element method, if no special stability treatment is used. Special stabilization techniques such as upwinding schemes or artificial viscosity are often used in the FVM and the FEM to discretize the original RTE. Another method

to overcome the stability problem just stated is to transform the original RTE into a second-order equation, in which the second-order derivative term can serve as an artificial viscosity to ensure stability of solution. Through parity decomposition of the radiative intensity, the even-parity formulation (EPF) of the RTE [30] was obtained, which is a second-order partial differential equation for the even parity of radiative intensity. It is well known that the second-order derivative term has the characteristic of diffusion and good numerical properties. Cheong and Song [31] examined several spatial discretization schemes in the DOM solution for the EPF of the RTE. Fiveland and Jessee [32, 33] studied the finite-element solution of the EFP of the RTE. Though the stability of the FEM solution of the second-order even-parity equation is ensured, numerical results indicate that the solution obtained using the FEM is less accurate as the optical thickness and the wall emissivity are increased.

In this article, by using a different transformation of the original RTE, a second-order radiative transfer equation (SORTE) with radiative intensity as primitive variable is derived, which has the major advantages of the EPF of the RTE but overcomes most of the drawbacks of it, and can be easily applied to solve radiative transfer in absorbing, emitting, and anisotropically scattering media. After examining the mathematical properties of the SORTE, we develop a finite-element method for solving multidimensional radiative transfer problems based on the discrete-ordinates equation of the SORTE. Four various test cases of radiative heat transfer in semitransparent media are used to verify the performance of the method.

FORMULATION OF THE SECOND-ORDER RADIATIVE TRANSFER EQUATION

The radiative transfer equation in an absorbing, emitting, and anisotropically scattering medium is

$$\frac{dI}{ds} + \beta I = \kappa_a I_b + \frac{\kappa_s}{4\pi} \int_{4\pi} I(s, \Omega') \Phi(\Omega', \Omega)\, d\Omega' \qquad s \in [0, L] \tag{1}$$

with the inflow boundary condition

$$I = I_0 \qquad s = 0 \tag{2}$$

where L is the length of the ray trajectory considered. If $\beta \neq 0$, Eq. (1) can be rewritten as

$$I = -\beta^{-1} \frac{dI}{ds} + (1 - \omega) I_b + \frac{\omega}{4\pi} \int_{4\pi} I(s, \Omega') \Phi(\Omega', \Omega)\, d\Omega' \tag{3}$$

Substituting Eq. (3) into the derivative term of Eq. (1) results in the following SORTE:

$$-\beta^{-1} \frac{d}{ds} \left(\beta^{-1} \frac{dI}{ds} \right) + I = S - \beta^{-1} \frac{dS}{ds} \tag{4}$$

where S is the source function, defined as

$$S = (1-\omega)I_b + \frac{\omega}{4\pi}\int_{4\pi} I(s,\Omega')\Phi(\Omega',\Omega)\,d\Omega' \tag{5}$$

When $\beta = 0$, the SORTE becomes

$$\frac{d^2I}{ds^2} = 0 \tag{6}$$

In the space of optical coordinates, the SORTE can be rewritten as

$$-\frac{d^2I}{d\tau^2} + I = S - \frac{dS}{d\tau} \qquad \tau \in [0, \tau_L] \tag{7}$$

where the optical coordinate τ and the optical thickness τ_L are defined, respectively, as

$$\tau = \int_0^s \beta(s)ds \qquad \tau_L = \int_0^L \beta(s)ds \tag{8}$$

In three-dimensional Cartesian coordinate, the second-order derivative term in the SORTE can be expanded as

$$\begin{aligned}\frac{d^2I}{d\tau^2} = {} & \mu^2\frac{\partial^2 I}{\partial\tau_x^2} + \eta^2\frac{\partial^2 I}{\partial\tau_y^2} + \xi^2\frac{\partial^2 I}{\partial\tau_z^2} + (\mu\eta+\eta\mu)\frac{\partial^2 I}{\partial\tau_x\partial\tau_y}(\mu\xi+\xi\mu)\frac{\partial^2 I}{\partial\tau_x\partial\tau_z} \\ & + (\eta\xi+\xi\eta)\frac{\partial^2 I}{\partial\tau_y\partial\tau_z}\end{aligned} \tag{9}$$

By substituting Eq. (9) into Eq. (7), we can see that the SORTE is a diffusion-type equation similar to the heat conduction equation of an anisotropic medium.

As shown in Eq. (7), the SORTE can be seen as a second-order ordinary differential equation (ODE) of radiative intensity with respect to the optical coordinate τ. It is known that two boundary conditions are needed to uniquely define a solution for the second ODE. Therefore, another appropriate boundary condition is needed to be imposed for the SORTE, besides the inflow boundary condition given by Eq. (2). A natural idea is to define a boundary condition for the outflow boundary of radiation. Because the original RTE describes radiative energy conservation and is valid at any position of ray trajectories, we can naturally use Eq. (1) as the outflow boundary condition for the SORTE, namely,

$$\beta^{-1}\frac{dI}{ds} + I = S \qquad s = L \tag{10}$$

In Cartesian coordinates, the SORTE given by Eq. (4) and boundary conditions Eq. (2) and Eq. (10) can be expressed in divergence form as

$$-\beta^{-1}\Omega\cdot\nabla[\beta^{-1}\Omega\cdot\nabla I] + I = S - \beta^{-1}\Omega\cdot\nabla S \tag{11}$$

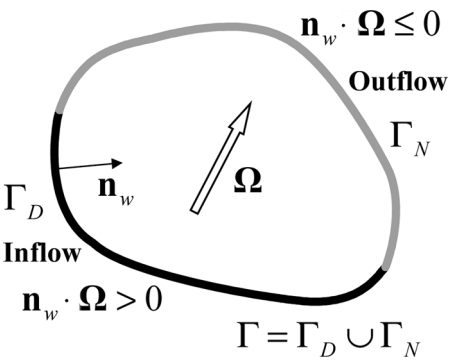

Figure 1. Schematic of boundary conditions for the second-order formula of the RTE.

$$I(\mathbf{r}_w, \Omega) = I_0(\mathbf{r}_w, \Omega) \qquad \mathbf{n}_w \cdot \Omega > 0 \tag{12a}$$

$$\beta^{-1}\Omega \cdot \nabla I + I = S \qquad \mathbf{n}_w \cdot \Omega \le 0 \tag{12b}$$

The boundary condition [Eq. (12*a*)] is conventionally called a Dirichlet boundary condition or essential boundary condition, and Eq. (12*b*) the Neumann boundary condition or natural boundary condition. A schematic of the boundary conditions for the SORTE is shown in Figure 1, where Γ denotes all the domain boundary with $\Gamma = \Gamma_D \cup \Gamma_N$; Γ_D and Γ_N denote the inflow boundary and the outflow boundary, respectively.

ANALYSIS OF MATHEMATICAL PROPERTIES OF THE SORTE

For the sake of analysis, the optical coordinate τ is normalized according to the optical thickness τ_L; then the original RTE can be rewritten as

$$\frac{1}{\tau_L}\frac{dI}{d\bar{\tau}} + I = S \qquad \bar{\tau} \in [0, 1] \tag{13}$$

Similarly, the SORTE given by Eq. (7) can be rewritten as

$$\frac{1}{{\tau_L}^2}\frac{d^2I}{d\bar{\tau}^2} + I = S - \frac{1}{\tau_L}\frac{dS}{d\bar{\tau}} \qquad \bar{\tau} \in [0, 1] \tag{14}$$

where $\bar{\tau}$ is the normalized optical coordinate, defined as

$$\bar{\tau} = \frac{\tau}{\tau_L} \tag{15}$$

The inflow and the outflow boundary conditions can be rewritten as

$$I = I_0 \qquad \bar{\tau} = 0 \tag{16a}$$

$$\frac{1}{\tau_L}\frac{dI}{d\bar{\tau}} + I = S \qquad \bar{\tau} = 1 \tag{16b}$$

Consistency

To check the consistency of the SORTE with the original RTE, we consider a radiative transfer problem in a nonemitting and nonscattering medium. For a nonemitting and nonscattering medium, the SORTE can be written as

$$-\frac{d^2I}{d\bar{\tau}^2} + \tau_L^2 I = 0 \tag{17}$$

with the inflow and the outflow boundary conditions

$$I = I_0 \qquad \bar{\tau} = 0 \tag{18a}$$

$$\frac{dI}{d\bar{\tau}} + \tau_L I = 0 \qquad \bar{\tau} = 1 \tag{18b}$$

The general solution of Eq. (17) can be found as

$$I(\bar{\tau}) = C_1 e^{-\tau_L \bar{\tau}} + C_2 e^{\tau_L \bar{\tau}} \tag{19}$$

The coefficients C_1 and C_2 are determined by the boundary conditions as $C_1 = I_0$ and $C_2 = 0$, respectively. Therefore, the solution of Eq. (17) can be written as

$$I(\bar{\tau}) = I_0 e^{-\tau_L \bar{\tau}} \qquad \bar{\tau} \in [0, 1] \tag{20}$$

which is the same as the solution of the original RTE with boundary condition given by Eq. (18*a*). This result proves the consistency of the SORTE with the RTE.

Perturbation Error Analysis

The solution of a physical model is often perturbed by errors of model parameters and boundary conditions. Thus, to know the spreading characteristics of the error is very important to evaluate the numerical properties of the SORTE.

First, we consider the perturbation error caused by inflow boundary condition. The perturbation error at the inflow boundary is simulated as a small constant perturbation in Eq. (16*a*), and written as

$$I = I_0 + \varepsilon \qquad \bar{\tau} = 0 \tag{21}$$

Under the boundary conditions given by Eq. (21) and Eq. (18*b*), the SORTE given by Eq. (17) has the following perturbed solution:

$$I_\varepsilon(\bar{\tau}) = (I_0 + \varepsilon) e^{-\tau_L \bar{\tau}} \tag{22}$$

Thus the relative perturbation error function of the solution is

$$E_{\text{in}}^{\text{rel}}(\bar{\tau}) = \frac{I_\varepsilon - I_E}{I_E} = \frac{\varepsilon e^{-\tau_L \bar{\tau}}}{I_0 e^{-\tau_L \bar{\tau}}} = \frac{\varepsilon}{I_0} \tag{23}$$

where I_E is the exact solution when no errors of model parameters and boundary conditions exist. From Eq. (23), it can be seen that the relative perturbation error is linearly proportional to the error at the inflow boundary and independent of the optical coordinates. For this inflow boundary condition perturbation, the relative perturbation error function is the same for the RTE.

Then we consider the perturbation errors caused by the outflow boundary condition. A small constant perturbation is imposed in the outflow boundary condition given by Eq. (18*b*) as follows:

$$\frac{dI}{d\bar{\tau}} + \tau_L I = \varepsilon \qquad \bar{\tau} = 1 \tag{24}$$

Under the boundary conditions given by Eq. (18*a*) and Eq. (24), the SORTE given by Eq. (17) has the following perturbed solution:

$$I_\varepsilon(\bar{\tau}) = I_0 e^{-\tau_L \bar{\tau}} + \frac{\varepsilon}{2\tau_L}\left[e^{-\tau_L(1-\bar{\tau})} - e^{-\tau_L(1+\bar{\tau})}\right] \qquad \bar{\tau} \in [0, 1] \tag{25}$$

In order to investigate the global property of the perturbation error in the solution of the SORTE, here we define the integral averaged relative error of the solution as

$$E^{\text{int}} = \frac{\int_0^1 |I_\varepsilon - I_E| d\bar{\tau}}{\int_0^1 |I_E| d\bar{\tau}} \tag{26}$$

By substituting the perturbed solution Eq. (25) and the exact solution into Eq. (26), we obtain the following integral averaged relative error for the solution of the SORTE caused by perturbation in the outflow boundary condition:

$$E_{\text{out}}^{\text{int}} = \frac{|\varepsilon|}{I_0} A_{\text{out}}(\tau_L) \tag{27}$$

where error amplifying factor $A_{\text{out}}(\tau_L)$ is

$$A_{\text{out}}(\tau_L) = \frac{1}{2\tau_L}(1 - e^{-\tau_L}) \tag{28}$$

As shown in Figure 2, the error amplifying factor $A_{\text{out}}(\tau_L)$ diminishes quickly with increasing of optical thickness and is always less than 1.0.

Finally, we consider the perturbation error caused by the radiative source function in the case of $S = 0$. The perturbed SORTE is written as

$$-\frac{d^2 I}{d\bar{\tau}^2} + \tau_L^2 I = \varepsilon \tag{29}$$

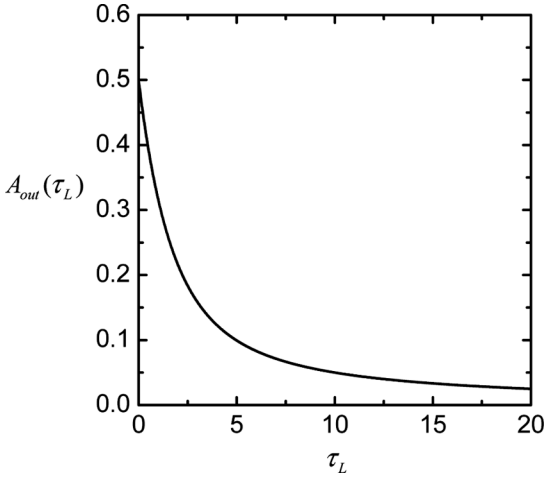

Figure 2. Error amplifying factor of outflow boundary condition.

and the integral averaged relative error is obtained by the same analysis procedure given above:

$$E^{\text{int}}_{S,2\text{nd}} = \frac{|\varepsilon|}{I_0} A_{S,2\text{nd}}(\tau_L) \tag{30}$$

where error amplifying factor $A_{S,2\text{nd}}(\tau_L)$ is

$$A_{S,2\text{nd}}(\tau_L) = \frac{1}{\tau_L}\left(\frac{1}{1-e^{-\tau_L}} - \frac{3-e^{-\tau_L}}{2\tau_L}\right) \tag{31}$$

The perturbation error caused by the radiative source function for the original RTE in the case of $S = 0$ can be similarly analyzed. The perturbed original RTE is written as

$$\frac{1}{\tau_L}\frac{dI}{d\bar{\tau}} + I = \varepsilon \qquad \bar{\tau} \in [0,1] \tag{32}$$

and the integral averaged relative error is obtained as

$$E^{\text{int}}_{S,1\text{st}} = \frac{|\varepsilon|}{I_0} A_{S,1\text{st}}(\tau_L) \tag{33}$$

where error amplifying factor $A_{S,1\text{st}}(\tau_L)$ is

$$A_{S,1\text{st}}(\tau_L) = \frac{1}{1-e^{-\tau_L}} - \frac{1}{\tau_L} \tag{34}$$

As shown in Figure 3, the amplifying factors $A_{S,1\text{st}}(\tau_L)$ and $A_{S,2\text{nd}}(\tau_L)$ are both not greater than 1.0. However, the amplifying factors $A_{S,1\text{st}}(\tau_L)$ of the original RTE increases with the optical thickness, but the amplifying factors $A_{S,2\text{nd}}(\tau_L)$ of the

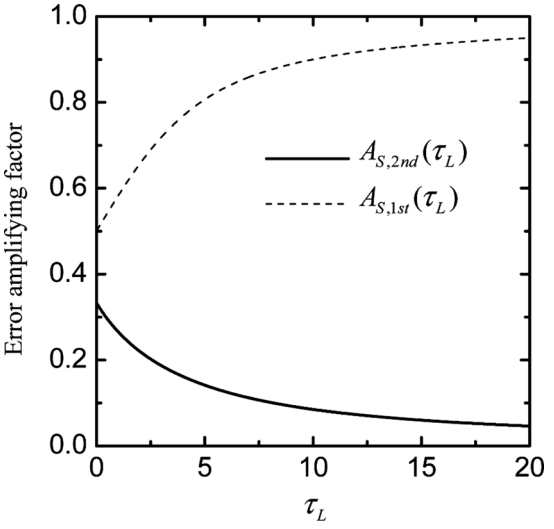

Figure 3. Comparison of error amplifying factors of radiative source term based on the SORTE and the original RTE.

SORTE diminish quickly with increasing optical thickness. From the above analysis, it can be seen that the SORTE has good numerical properties.

NUMERICAL SOLUTION METHOD

In order to fully verify the second-order formula for the RTE and the associated boundary conditions described above, a numerical solution method based on the Galerkin finite-element method is developed to solve the SORTE. First, the discrete-ordinates equation of the SORTE is formulated, and then a general formulation of Galerkin discretization is derived based on the discrete-ordinates equation. Finally, the implementation of boundary conditions and solution procedure is presented.

Discrete-Ordinates Equation

Here, the discrete-ordinates method is used for the angular discretization. Equations (11) and (12) are replaced by a set of equations for the discrete directions. The resulting discrete-ordinates equations of the SORTE with boundary conditions can be written as

$$-\beta^{-1}\Omega^m \cdot \nabla[\beta^{-1}\Omega^m \cdot \nabla I(\mathbf{r},\Omega^m)] + I(\mathbf{r},\Omega^m) = S(\mathbf{r},\Omega^m) - \beta^{-1}\Omega^m \cdot \nabla S(\mathbf{r},\Omega^m) \quad (35)$$

$$I(\mathbf{r}_w,\Omega^m) = I_0(\mathbf{r}_w,\Omega^m) \qquad \mathbf{n}_w \cdot \Omega > 0 \quad (36a)$$

$$\beta^{-1}\Omega^m \cdot \nabla I(\mathbf{r}_w,\Omega^m) + I(\mathbf{r}_w,\Omega^m) = S(\mathbf{r}_w,\Omega^m) \qquad \mathbf{n}_w \cdot \Omega \le 0 \quad (36b)$$

For the opaque, diffuse emitting and reflecting wall, the inflow boundary condition is

$$I_0(\mathbf{r}_w, \Omega^m) = \varepsilon_w I_b(\mathbf{r}_w) + \frac{1-\varepsilon_w}{\pi} \sum_{\mathbf{n}_w \cdot \Omega^{m'} < 0} I(\mathbf{r}_w, \Omega^{m'}) |\mathbf{n}_w \cdot \Omega^{m'}| w^{m'} \tag{37}$$

where Ω^m is the discrete angular direction, $w^{m'}$ is the weight corresponding to direction m', and $\mathbf{n}_w$ is inward normal vector of the boundary.

Galerkin Discretization

By multiplying by β, Eq. (35) can be written as

$$-\Omega^m \cdot \nabla[\beta^{-1}\Omega^m \cdot \nabla I^m] + \beta I^m = \beta S^m - \Omega^m \cdot \nabla S^m \tag{38}$$

The advantage of replacing Eq. (35) by Eq. (38) for Galerkin discretization is that the resulting stiff matrix is always symmetric even if β is a function of spatial coordinates. Weighting Eq. (38) by shape function ϕ_j and then integrating over the solution domain yields

$$\begin{aligned} &\langle \beta^{-1}\Omega^m \cdot \nabla I^m, \Omega^m \cdot \nabla \phi_j \rangle + \int_\Gamma \beta^{-1}\Omega^m \cdot \nabla I^m \phi_j (\Omega^m \cdot \mathbf{n}_w)\, dA + \langle \beta I^m, \phi_j \rangle \\ &= \langle \beta S^m, \phi_j \rangle - \langle \Omega^m \cdot \nabla S^m, \phi_j \rangle \end{aligned} \tag{39}$$

where Γ denotes the boundary of solution domain with $\Gamma = \Gamma_D \cup \Gamma_N$; Γ_D and Γ_N denote the inflow and the outflow boundaries as shown in Figure 1. The inner product $\langle \cdot, \cdot \rangle$is defined as

$$\langle f, g \rangle = \int_V fg\, dV \tag{40}$$

If we choose $\phi_j \in U_D := \{u(\mathbf{r}) | u(\mathbf{r}) = 0, \mathbf{r} \in \Gamma_D\}$, then Eq. (39) can be written as

$$\begin{aligned} &\langle \beta^{-1}\Omega^m \cdot \nabla I^m, \Omega^m \cdot \nabla \phi_j \rangle + \int_{\Gamma_N} \beta^{-1}\Omega^m \cdot \nabla I^m \phi_j (\Omega^m \cdot \mathbf{n}_w)\, dA + \langle \beta I^m, \phi_j \rangle \\ &= \langle \beta S^m, \phi_j \rangle - \langle \Omega^m \cdot \nabla S^m, \phi_j \rangle \end{aligned} \tag{41}$$

From the outflow boundary condition given by Eq. (36*b*), we have

$$\int_{\Gamma_N} \beta^{-1}\Omega^m \cdot \nabla I^m \phi_j (\Omega^m \cdot \mathbf{n}_w)\, dA = \int_{\Gamma_N} (S^m - I^m) \phi_j (\Omega^m \cdot \mathbf{n}_w)\, dA \tag{42}$$

Substituting Eq. (42) into Eq. (41) leads to

$$\begin{aligned} &\langle \beta^{-1}\Omega^m \cdot \nabla I^m, \Omega^m \cdot \nabla \phi_j \rangle - \int_{\Gamma_N} I^m \phi_j (\Omega^m \cdot \mathbf{n}_w)\, dA + \langle \beta I^m, \phi_j \rangle \\ &= \langle \beta S^m, \phi_j \rangle - \langle \Omega^m \cdot \nabla S^m, \phi_j \rangle - \int_{\Gamma_N} S^m \phi_j (\Omega^m \cdot \mathbf{n}_w)\, dA \end{aligned} \tag{43}$$

Using the shape function approximation of radiative intensity, namely,

$$I^m(\mathbf{r}) \simeq \sum_{i=1}^{N_{\text{sol}}} I_i^m \phi_i(\mathbf{r}) \tag{44}$$

Eq. (43) can be written in matrix form for each discrete direction Ω^mas

$$\mathbf{K}^m \mathbf{I}^m = \mathbf{H}^m \tag{45}$$

where the stiff matrix $\mathbf{K}^m$ and the right-hand-side vector $\mathbf{H}^m$ are defined, respectively, as

$$K_{ji}^m = \langle \beta^{-1} \Omega^m \cdot \nabla \phi_i, \Omega^m \cdot \nabla \phi_j \rangle - \int_{\Gamma_N} \phi_i \phi_j (\Omega^m \cdot \mathbf{n}_w)\, dA + \langle \beta \phi_i, \phi_j \rangle \tag{46}$$

$$H_j^m = \langle \beta S^m, \phi_j \rangle - \langle \Omega^m \cdot \nabla S^m, \phi_j \rangle - \int_{\Gamma_N} S^m \phi_j (\Omega^m \cdot \mathbf{n}_w)\, dA \tag{47}$$

From Eq. (46), it can be seen that the Galerkin discretization of the SORTE ensures a symmetric stiff matrix for every discrete ordinate direction, which is a good numerical property.

Implementation

The outflow boundary conditions have been imposed implicitly in the Galerkin discretization formulation by using the Gauss theorem. Here, we use the collocation technique [34, 35] to impose the inflow boundary condition, that is, for each node j on the inflow boundary of direction Ω^m described by Eq. (36*a*), the matrix $\mathbf{K}^m$ and the vector $\mathbf{H}^m$ are modified as follows:

$$K_{ji}^m = \begin{cases} 1 & j = i \\ 0 & j \neq i \end{cases} \tag{48a}$$

$$H_j^m = I_j^m \tag{48b}$$

In the following analysis, a finite-element method implementation of the Galerkin discretization of the SORTE is employed. The implementation of the method is carried out according to the following routine.

Step 1. Mesh the solution domain with N_{el} nonoverlapping elements.
Step 2. Loop each angular direction for $m = 1, \ldots, M$, then assemble the global stiff matrix $\mathbf{K}^m$, and the right-hand-side vector $\mathbf{H}^m$.
Step 3. Modify $\mathbf{K}^m$ and $\mathbf{H}^m$ to impose the inflow boundary condition according to Eq. (48).
Step 4. Solving the linear equation given by Eq. (45) to get the radiative intensity on each node for discrete ordinate direction m.

Step 5. Terminate the iteration process if the stop criterion is met. Otherwise go back to Step 2.

In this article, the maximum relative error 10^{-4} of incident radiation is taken as the stopping criterion for the global iteration.

RESULTS AND DISCUSSION

Computer code has been developed based on the numerical methods described above. To verify the formulations presented in this article, four various test cases are selected to fully verify the performance of the SORTE. For the sake of analysis and comparison, the integral averaged relative error is defined as

$$\text{Relative error } \% = \frac{\int_V |\text{numerial solution} - \text{exact value}|\, dV}{\int_V |\text{exact value}|\, dV} \times 100 \tag{49}$$

Case 1: Gaussian-Shaped Radiative Source Term between One-Dimensional Parallel Black Slabs

We consider the radiative transfer problems in a nonscattering medium between one-dimensional infinite parallel black slabs. The radiative source term of the medium has a profile similar to a Gaussian function. This problem is modeled by the following RTE as

$$\mu \frac{dI}{dx} + \kappa_a I = e^{-(x-c)^2/\alpha^2} \qquad x, c \in [0,1] \tag{50}$$

with the boundary conditions

$$I(0,\mu) = \kappa_a^{-1} e^{-c^2/\alpha^2} \qquad \mu > 0 \tag{51a}$$

$$I(1,\mu) = \kappa_a^{-1} e^{-(1-c)^2/\alpha^2} \qquad \mu < 0 \tag{51b}$$

The analytical solution of this problem in the case of $\mu > 0$ can be written as

$$I(x,\mu) = I(0,\mu)\exp\left(-\frac{\kappa_a x}{\mu}\right) - \frac{\alpha\sqrt{\pi}}{2\mu}\exp\left\{-\frac{\kappa_a}{\mu}\left[x - \left(\frac{\alpha^2\kappa_a}{4\mu} + c\right)\right]\right\}\left[\operatorname{erf}\left(\frac{\alpha\kappa_a}{2\mu} + \frac{c-x}{\alpha}\right) - \operatorname{erf}\left(\frac{\alpha\kappa_a}{2\mu} + \frac{c}{\alpha}\right)\right] \tag{52}$$

The FEM based on the SORTE is applied to the case of $c = 0.5$, $\alpha = 0.02$, in which 50 linear isoparametric elements are used. The distribution of radiative intensity in the direction of $\mu = 0.5773503$ is presented in Figure 4 for three different optical thicknesses, 0.1, 1, and 10, and compared to the analytical solution. The results obtained by the Galerkin FEM based on the original RTE with the same

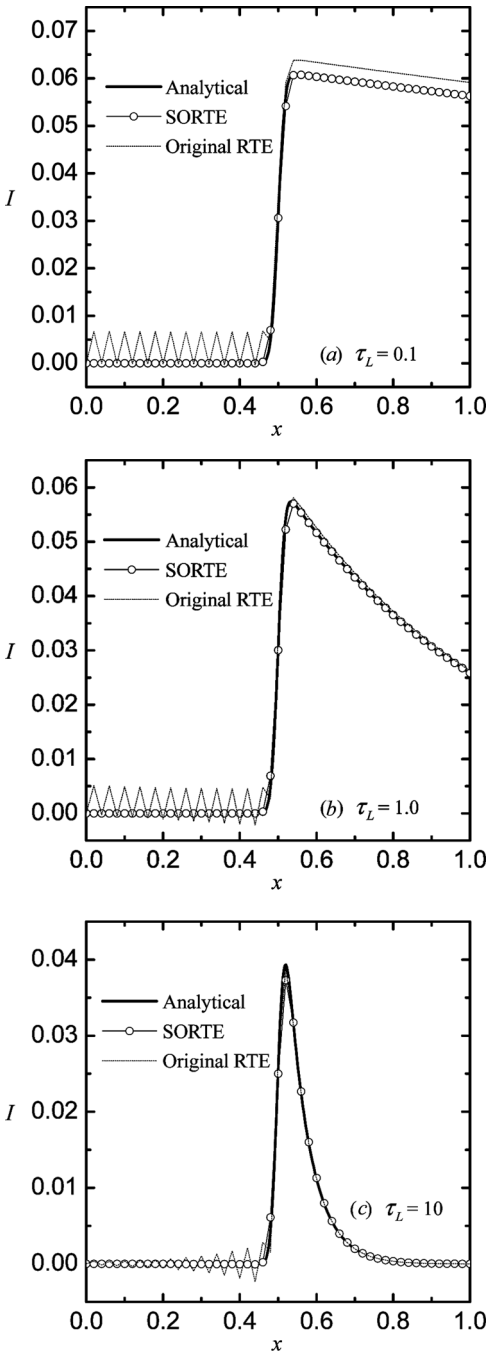

Figure 4. Distribution of radiative intensity in a one-dimensional slab: (*a*) $\tau_L = 0.1$; (*b*) $\tau_L = 1.0$; (*c*) $\tau_L = 10$.

spatial grid are also presented as a comparison. It can be seen that the results obtained using the SORTE are accurate and stable for all three optical thicknesses, while the results obtained using the original RTE exhibit obvious nonphysical oscillations, though the oscillations diminish with increasing optical thickness.

Case 2: Isotropic Scattering in a Gray Enclosure

In this case, a square enclosure filled by isotropically scattering medium with single albedo $\omega = 1.0$ is considered. The bottom wall of the enclosure is kept hot and its temperature is denoted as T_{w1}, but all other walls and the medium bounded by the enclosure are kept cold. The FEM based on the SORTE is applied to this case with 400 linear quadrilateral isoparametric elements, in which the S_8 approximation is used for discrete-ordinates discretization. The dimensionless net radiative heat fluxes $q_w/\sigma T_{w1}^4$ along the hot wall are presented in Figure 5 for three different values of wall emissivities, $\varepsilon_w = 0.1, 0.5$, and 1.0, and compared to the results obtained using the zone method [36]. It can be seen that the results obtained using the SORTE agree with those obtained using the zone method very well. The integral averaged relative error based on the results obtained using the zone method for the case of $\varepsilon_w = 1.0$ is less than 1%. Figure 6 shows a comparison of results obtained using the FEM based the SORTE and the original RTE in the case of $\varepsilon_w = 0.5$. It can be seen that obvious nonphysical oscillations still exist in the results obtained using the FEM based on the original RTE.

Case 3: Anisotropic Scattering in a Black Enclosure

In this case, we consider the radiative heat transfer problem in a gray medium enclosed by a square black enclosure. The optical thickness based on the side length L of the enclosure is $\tau_L = \beta L = 1.0$. The medium is kept hot, but all the boundary

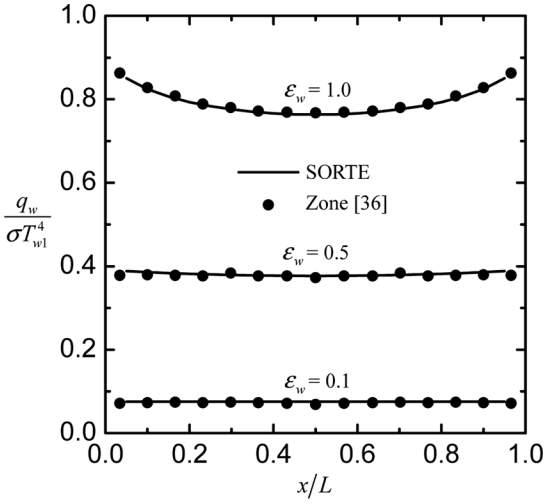

Figure 5. Distribution of dimensionless net radiative heat fluxes along the bottom wall of a gray enclosure.

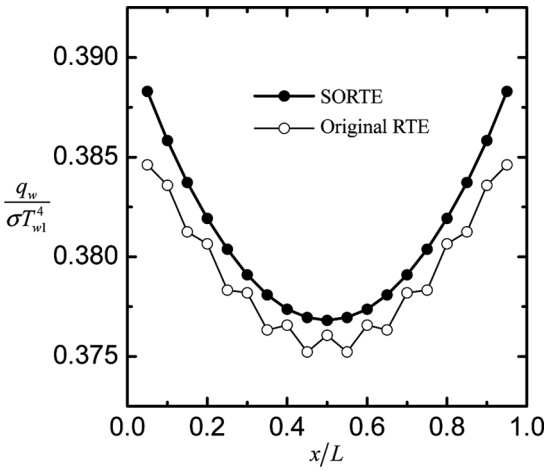

Figure 6. Comparison of dimensionless net radiative heat fluxes obtained using the SORTE and the original RTE in the case of $\varepsilon_w = 0.5$.

walls are kept cold. The temperature T_g, the absorption coefficient, and the scattering coefficient of the medium bounded by the enclosure are uniform. The following scattering phase function [38] with asymmetry factor of 0.66972 is used:

$$\Phi = \sum_{j=0}^{8} C_j P_j(\mu) \tag{53}$$

where the P_j are the Legendre polynomials. The C_j are the expansion coefficients defined as $C_0 = 1.0$, $C_1 = 2.00917$, $C_2 = 1.56339$, $C_3 = 0.67407$, $C_4 = 0.22215$, $C_5 = 0.04725$, $C_6 = 0.00671$, $C_7 = 67407$, and $C_8 = 0.00005$, respectively.

The FEM based on the SORTE is applied to this case with 400 linear quadrilateral isoparametric elements, in which the S_8 approximation is used for discrete-ordinates discretization. The dimensionless net radiative heat fluxes $(q_w/\sigma T_g^4)$ on the lower wall for three different single scattering albedos, $\omega = 0.0, 0.5$, and 0.9, are shown in Figure 7 and compared to the results obtained using the DOM [37]. The integral averaged relative error based on the DOM data in [37] is less than 0.9% for the case of $\omega = 0.5$. The FEM based on the SORTE has good accuracy in solving the radiative heat transfer problems in an anisotropically scattering medium.

Case 4: Nonscattering Medium in a Semicircular Enclosure with a Circular Hole

As shown in Figure 8*a*, we consider a semicircle enclosure with a circular hole. The medium is kept hot, while all boundaries are black and kept cold. The temperature T_g and the absorption coefficient of the medium bounded by the enclosure are uniform. The FEM based on the SORTE is applied to this case with 450 linear quadrilateral isoparametric elements, in which the S_8 approximation is used for discrete-ordinates discretization. The elements distribution is shown in Figure 8*b*.

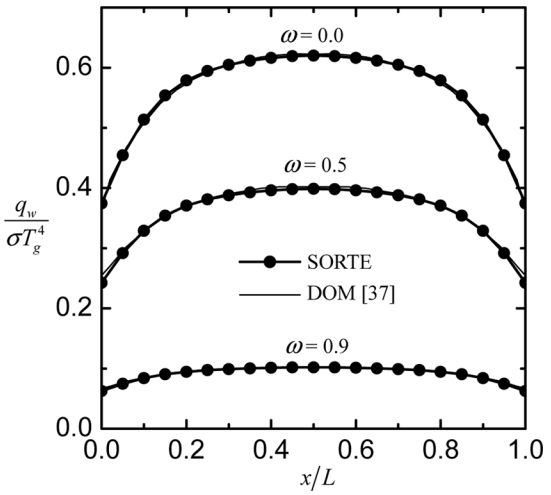

Figure 7. Distribution of dimensionless net radiative heat fluxes on the bottom wall of a square enclosure filled with an anisotropically scattering medium.

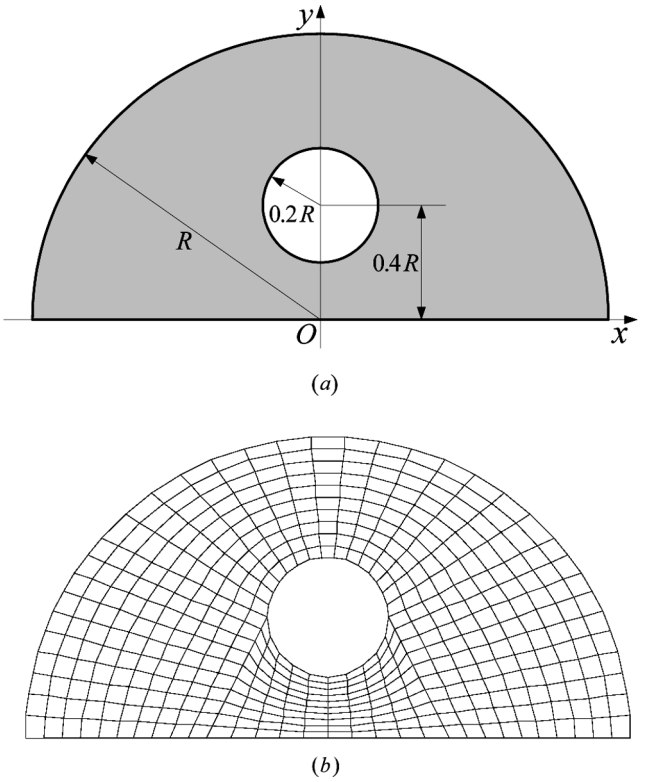

Figure 8. Semicircle enclosure with a circular hole: (*a*) configuration; (*b*) mesh with 450 elements.

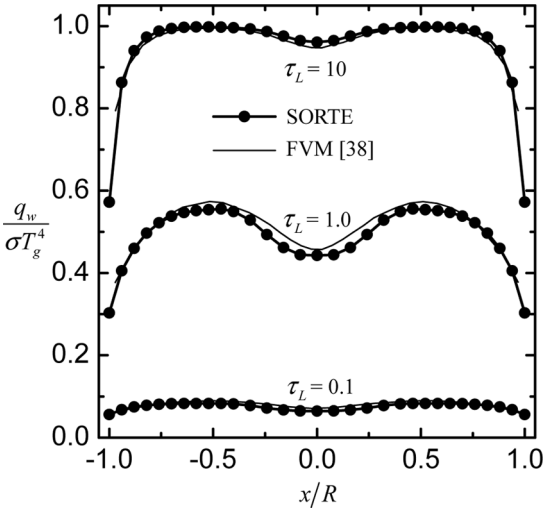

Figure 9. Distribution of dimensionless net radiative heat flux along the bottom wall of a semicircle enclosure.

The distribution of the dimensionless net radiative heat flux $q_w/\sigma T_g^4$ along the bottom wall are presented in Figure 9 for three different optical thicknesses ($\tau_L = \beta R$), namely, 0.1, 1.0, and 10, and compared to the results obtained using the FVM [38]. It can be seen that the results obtained using the FEM based on the SORTE agree well with the FVM data in [38]. The integral averaged relative error based on the FVM data for the case of $\tau_L = 1.0$ is less than 3%. The FEM based on the SORTE developed in this article has good accuracy in solving radiative heat transfer problems with complex geometric configurations.

CONCLUSIONS

A second-order radiative transfer equation (SORTE) has been derived for an absorbing, emitting, and anisotropically scattering medium. This new equation is a diffusion-type equation similar to the heat conduction equation for an anisotropic medium. The appropriate boundary conditions for the SORTE have been discussed. The consistency of the SORTE under the given boundary conditions with the original RTE has been demonstrated. The perturbation characteristics of the error in the boundary conditions and the radiative source term have been analyzed for both the SORTE and the original RTE. Good numerical properties have been found for the SORTE. A general formulation of Galerkin discretization based on the discrete-ordinates equation of the SORTE has been derived, which guided a symmetric stiff matrix for every discrete ordinate direction. A finite-element method implementation of the Galerkin discretization of the SORTE has been employed to solve radiative heat transfer problems in multidimensional semitransparent media. Four various test problems were taken as examples to verify the formulations. The predicted radiative intensity distributions and net radiative heat flux determined by the FEM based on

the SORTE agree very well with the analytical solutions and data in references. Results show that the FEM based on the SORTE is numerically stable, efficient, and accurate for solving radiative transfer problems in semitransparent media.

REFERENCES

1. H. C. Hottel and E. S. Cohen, Radiant Heat Exchange in a Gas-Filled Enclosure Allowance for Nonuniformity of Gas Temperature, *AIChE J.*, vol. 4, pp. 3–14, 1958.
2. J. R. Howell, Application of Monte Carlo to Heat Transfer Problems, *Adv. Heat Transfer*, vol. 5, pp. 1–54, 1968.
3. M. F. Modest, *Radiative Heat Transfer*, McGraw-Hill, New York, 1993.
4. W. A. Fiveland, Discrete-Ordinates Solution of the Radiative Transport Equation for Rectangular Enclosures, *ASME J. Heat Transfer*, vol. 106, pp. 699–706, 1984.
5. J. C. Chai, H. O. Lee, and S. V. Patankar, Ray Effect and False Scattering in the Discrete Ordinates Method, *Numer. Heat Transfer B*, vol. 24, pp. 373–389, 1993.
6. J. C. Chai, H. S. Lee, and S. V. Patankar, Improved Treatment of Scattering Using the Discrete Ordinates Method, *J. Heat Transfer*, vol. 116, pp. 260–263, 1994.
7. F. Liu, H. A. Becker, and A. Pollard, Spatial Differencing Schemes of the Discrete-Ordinates Method, *Numer. Heat Transfer B*, vol. 30, pp. 23–43, 1996.
8. S. W. Baek and M. Y. Kim, Modification of the Discrete-Ordinates Method in an Axisymmetric Cylindrical Geometry, *Numer. Heat Transfer B*, vol. 31, pp. 313–326, 1997.
9. J. Con and P. J. Coelho, Parallelization of the Discrete Ordinates Method, *Numer. Heat Transfer B*, vol. 32, pp. 151–173, 1997.
10. S. H. Kim and K. Y. Huh, Assessment of the Finite-Volume Method and the Discrete Ordinate Method for Radiative Heat Transfer in a Three-Dimensional Rectangular Enclosure, *Numer. Heat Transfer B*, vol. 35, pp. 85–112, 1999.
11. K. H. Lee and R. Viskanta, Two-Dimensional Combined Conduction and Radiation Heat Transfer: Comparison of the Discrete Ordinates Method and the Diffusion Approximation Methods, *Numer. Heat Transfer A*, vol. 39, pp. 205–225, 2001.
12. N. Sel and G. Kirbas, The Method of Lines Solution of the Discrete Ordinates Method for Radiative Heat Transfer in Enclosures, *Numer. Heat Transfer B*, vol. 37, pp. 379–392, 2000.
13. N. Sel and I. Ayranci, The Method of Lines Solution of the Discrete Ordinates Method for Radiative Heat Transfer in Enclosures Containing Scattering Media, *Numer. Heat Transfer B*, vol. 43, pp. 179–201, 2003.
14. H. S. Li, G. Flamant, and J. D. Lu, Mitigation of Ray Effects in the Discrete Ordinates Method, *Numer. Heat Transfer B*, vol. 43, pp. 445–466, 2003.
15. G. Krishnamoorthy, R. Rawat, and P. J. Smith, Parallel Computations of Radiative Heat Transfer Using the Discrete Ordinates Method, *Numer. Heat Transfer B*, vol. 47, pp. 19–38, 2005.
16. G. D. Raithby and E. H. Chui, A Finite-Volume Method for Predicting a Radiant Heat Transfer in Enclosures with Participating Media, *ASME J. Heat Transfer*, vol. 112, pp. 415–423, 1990.
17. J. C. Chai and H. S. Lee, Finite-Volume Method for Radiation Heat Transfer, *J. Thermophys. Heat Transfer*, vol. 8, pp. 419–425, 1994.
18. J. C. Chai, H. O. Lee, and S. V. Patankar, Treatment of Irregular Geometries Using a Cartesian Coordinates Finite-Volume Radiation Heat Transfer Procedure, *Numer. Heat Transfer B*, vol. 26, pp. 225–235, 1994.
19. J. Y. Murthy and S. R. Mathur, Finite Volume Method for Radiative Heat Transfer Using Unstructured Meshes, *J. Thermophys. Heat Transfer*, vol. 12, pp. 313–321, 1998.

20. G. D. Raithby, Discussion of the Finite-volume Method for Radiation, and Its Application Using 3D Unstructured Meshes, *Numer. Heat Transfer B*, vol. 35, pp. 389–405, 1999.
21. J. C. Chai and S. V. Patankar, Finite-Volume Method for Radiation Heat Transfer, *Adv. Numer. Heat Transfer*, vol. 2, pp. 109–141, 2000.
22. J. C. Chai, One-Dimensional Transient Radiation Heat Transfer Modeling Using a Finite-Volume Method, *Numer. Heat Transfer B*, vol. 44, pp. 187–208, 2003.
23. K. Slimi, L. Zili-Ghedira, N. S. Ben, and A. A. Mohamad, A Transient Study of Coupled Natural Convection and Radiation in a Porous Vertical Channel Using the Finite-Volume Method, *Numer. Heat Transfer A*, vol. 45, pp. 451–478, 2004.
24. M. Lobo and A. F. Emery, Discrete Maximum Principle in Finite-Element Thermal Radiation Analysis, *Numer. Heat Transfer B*, vol. 24, pp. 209–227, 1993.
25. J. V. Daurelle, R. Occelli, and R. Martin, Finite-Element Modeling of Radiation Heat Transfer Coupled with Conduction in an Adaptive Method, *Numer. Heat Transfer B*, vol. 25, pp. 61–73, 1994.
26. V. B. Kisslelev, L. Roberti, and G. Perona, An Application of the Finite-Element Method to the Solution of the Radiative Transfer Equation, *J. Quant. Spectrosc. Radiat. Transfer*, vol. 51, pp. 603–614, 1994.
27. L. H. Liu, Finite Element Simulation of Radiative Heat Transfer in Absorbing and Scattering Media, *J. Thermophys. Heat Transfer*, vol. 18, pp. 555–557, 2004.
28. X. Cui and B. Q. Li, A Discontinuous Finite-Element Formulation for Internal Radiation Problems, *Numer. Heat Transfer B*, vol. 46, pp. 223–242, 2004.
29. J. P. Pontaza and J. N. Reddy, Least-Squares Finite Element Formulations for One-Dimensional Radiative Transfer, *J. Quant. Spectrosc. Radiat. Transfer*, vol. 95, pp. 387–406, 2005.
30. E. E. Lewis and W. F. Miller, *Computational Methods of Neutron Transport*, Wiley, New York, 1984.
31. K. B. Cheong and T. H. Song, Examination of Solution Methods for the Second-Order Discrete Ordinate Formulation, *Numer. Heat Transfer B*, vol. 27, pp. 155–173, 1995.
32. W. A. Fiveland and J. P. Jessee, Finite Element Formulation of the Discrete-Ordinates Method for Multidimensional Geometries, *J. Thermophys. Heat Transfer*, vol. 8, pp. 426–433, 1994.
33. W. A. Fiveland and J. P. Jessee, Comparison of Discrete Ordinates Formulations for Radiative Heat Transfer in Multidimensional Geometries, *J. Thermophys. Heat Transfer*, vol. 9, pp. 47–54, 1995.
34. L. H. Liu, Meshless Local Petrov-Galerkin Method for Solving Radiative Transfer Equation, *J. Thermophys. Heat Transfer*, vol. 20, pp. 150–154, 2005.
35. J. M. Zhao and L. H. Liu, Least-Squares Spectral Element Method for Radiative Heat Transfer in Semitransparent Media, *Numer. Heat Transfer B*, vol. 50, pp. 473–489, 2006.
36. A. C. Ratzel and J. R. Howell, Two-Dimensional Radiation in Absorbing-Emitting Media Using the P-N Approximation, *ASME J. Heat Transfer*, vol. 105, pp. 333–340, 1983.
37. T. K. Kim and H. Lee, Effect of Anisotropic Scattering on Radiative Heat Transfer in Two-Dimenssional Rectangular Enclosures, *Int. J. Heat Mass Transfer*, vol. 31, pp. 1711–1721, 1988.
38. M. Y. Kim, S. W. Baek, and J. H. Park, Unstructured Finite-Volume Method for Radiative Heat Transfer in a Complex Two-Dimensional Geometry with Obstacles, *Numer. Heat Transfer B*, vol. 39, pp. 617–635, 2001.